J. Fluid Mech. (1972), *vol.* 56, *part* 2, *pp.* 313–336
Printed in Great Britain

Statistical hydromechanics of disperse systems. Part 3. Pseudo-turbulent structure of homogeneous suspensions

By YU. A. BUYEVICH
Institute for Problems in Mechanics, USSR Academy of Sciences, Moscow

(Received 8 March 1972)

The theory of concentrated two-phase mixtures developed in the previous parts of this paper is applied to analysis of the structure of the local random motion (pseudo-turbulence) occurring in flows of suspensions of small solid spheres. Suspensions under study are assumed to be locally homogeneous in the sense that large-scale agglomerates of many particles or voids filled with the pure liquid do not arise in their flows and particles can be approximately regarded as statistically independent units.

Coefficients of the particle diffusion caused by pseudo-turbulence are calculated without restrictions imposed on the value of the Reynolds number Re characterizing the fluid flow around one particle. Other pseudo-turbulent quantities (the r.m.s. pseudo-turbulent velocities of both phases, their effective pseudo-turbulent viscosities in a shear flow, etc.) are considered for small Re. In particular, a natural explanation is given to the known effect of the reduced hydraulic resistance of a fluidized bed as compared with that of a stationary particulate bed of the same porosity.

Additionally, some properties of the mean motion of a suspension influenced by pseudo-turbulence are discussed brifly. By way of example, two problems are considered: stability of the upward flow of a homogeneous suspension with respect to small perturbations depending upon the vertical co-ordinate and time, and the spatial distribution of particles suspended by the upward flow of a fluid under gravity.

1. Introduction

As follows from the theory in the first parts of this paper (Buyevich 1971, 1972, henceforth denoted by I and II respectively), the pseudo-turbulent motion of particles and a fluid represents an inherent property of any disperse system and influences its 'macroscopic' mean motion. The immediate objective of this part is to illustrate the general theory suggested in I and II by considering some particular examples of its application both to analysis of statistical properties of pseudo-turbulence in a given state of a disperse system and to investigation of the macroscopic behaviour of this system under certain external conditions. Obviously, this objective agrees well with two primary aims of the theory itself, formulated in I. It goes without saying, of course, that results of such a

treatment may be of independent interest for various particular problems concerning the disperse system under study.

Experiments as well as certain estimates based upon the theory in I show that flow patterns of two different types are possible within real flows of a disperse system. First, there are situations when the microscopic structure of a flow is locally homogeneous, so that suspended particles behave on an average like statistically independent elements. Second, in some flows (e.g. in fluidized beds of coarse particles) agglomerates containing a large number of particles or, on the other hand, macroscopic voids filled with pure suspending fluid can appear, i.e. there exists an essential interaction between neighbouring particles. For the sake of simplicity, here we confine ourselves to investigation of locally homogeneous flows, employing all the assumptions, restrictions and notation introduced previously in I and II.

The real velocities of the fluid and particles, the pressure and the volume concentration of a monodisperse suspension are $\langle \mathbf{v} \rangle + \mathbf{v}'$, $\langle \mathbf{w} \rangle + \mathbf{w}'$, $\langle p \rangle + p'$ and $\langle \rho \rangle + \rho'$, respectively. The first terms of these expressions denote the corresponding dynamic quantities and are related to the mean motion of both phases looked upon as two co-existing continua. The second terms are the pseudo-turbulent random pulsations, which can be represented in the form of Fourier–Stieltjes integrals, i.e.

$$\mathbf{v}' = \int e^{i(\omega t + \mathbf{kr})} d\mathbf{Z}_v, \quad \mathbf{w}' = \int e^{i(\omega t + \mathbf{kr})} d\mathbf{Z}_w, \quad \text{etc.}$$

Stochastic equations for these random processes have been derived in I from the Langevin equation for one particle and modified Navier–Stokes equations governing flow of the fluid through a random lattice formed by all suspended particles. From the stochastic equations mentioned one easily obtains the following equations for the spectral measures appearing in the Fourier–Stieltjes representations of the random processes under study:

$$\left.\begin{aligned}
&(\omega + \mathbf{uk})\, dZ_\rho - \epsilon \mathbf{k}\, d\mathbf{Z}_v = 0, \quad i d_1 \rho \omega\, d\mathbf{Z}_w = d\mathbf{Z}_F, \quad \epsilon = 1 - \rho, \\
&i d_0 \epsilon(\omega + \mathbf{uk})\, d\mathbf{Z}_v = -i\mathbf{k}\, dZ_p - \mu_0 S[k^2 d\mathbf{Z}_v + \tfrac{1}{3}\mathbf{k}(\mathbf{k}\, d\mathbf{Z}_v)] - d\mathbf{Z}_F, \\
&d\mathbf{Z}_F = -i\rho \mathbf{k}\, dZ_p + d_0 \rho \Big[(\beta_1 K_1 + \beta_2 K_2 u)\, d\mathbf{Z}_u + \beta_2 K_2 (\mathbf{u}_0\, d\mathbf{Z}_u)\, \mathbf{u} \\
&\qquad + \left(\beta_1 \frac{dK_1}{d\rho} + \beta_2 \frac{dK_2}{d\rho} u + i\omega \frac{d\eta}{d\rho} \right) \mathbf{u}\, dZ_\rho \Big], \quad \mathbf{u} = \mathbf{v} - \mathbf{w}, \quad \mathbf{u}_0 = \mathbf{u}/u.
\end{aligned}\right\} \tag{1.1}$$

The meaning of quantities involved in (1.1) is clear from I; to simplify the nomenclature, the pointed brackets around the symbols for the dynamic quantities describing the mean motion of both phases are dropped. Here $S = S(\rho)$ is a function defining the effective viscosity $\mu = \mu_0 S(\rho)$ of the fluid filtering through the lattice of particles, which differs from the fluid molecular viscosity μ_0; d_0 and d_1 are the densities of the fluid and the particle substance. Quantities involved in the relation for the spectral measure $d\mathbf{Z}_F$ of the random pulsation of the interphase interaction force in (1.1) (in particular, those depending on the particle radius a) are specified by equations (1.2)–(1.4) below. Note that equations (1.1)

are related to the equilibrium state of a disperse system when $\mathbf{v}$, $\mathbf{w}$ and ρ do not depend upon the space co-ordinates or time.

Expressions for β_1 and β_2 and K_1 and K_2 follow from an equation for the stationary drag force $\mathbf{F}_d$ experienced by suspended particles inside a unit volume of the mixture. Such an equation can be in principle obtained theoretically or on the basis of experiments. Below we use Ergun's (1952) semi-empirical relation

$$\left.\begin{aligned} &\mathbf{F}_d = d_0\rho(\beta_1 K_{1d} + \beta_2 K_{2d} u_f)\,\mathbf{u}_f, \quad \mathbf{u}_f = \epsilon\mathbf{u}, \\ &\beta_1 = \frac{9}{2}\frac{\nu_0}{a^2}, \quad \beta_2 = \frac{1{\cdot}75}{2a}, \quad K_{1d} = \frac{25}{3}\frac{\rho}{\epsilon^3}, \quad K_{2d} = \frac{1}{\epsilon^2}, \quad \nu_0 = \frac{\mu_0}{d_0}. \end{aligned}\right\} \tag{1.2}$$

The force given in (1.2) satisfies the relation

$$-\nabla p + d_0\mathbf{g} - \mathbf{F}_d = 0.$$

On the other hand, the corresponding relation including K_1 and K_2 instead of K_{1d} and K_{2d} follows from the equation of momentum conservation for the fluid phase in the stationary homogeneous flow and has the form

$$\epsilon(-\nabla p + d_0\mathbf{g}) - d_0\rho(\beta_1 K_1 + \beta_2 K_2 u)\mathbf{u} = 0.$$

By comparing these relations we get from (1.2)

$$K_1 = K = \epsilon^2 K_{1d} = 25\rho(3\epsilon)^{-1}, \quad K_2 = \epsilon^2 K_{2d} = 1. \tag{1.3}$$

It is essential that Ergun's formula (1.2) as well as (1.3) is valid for

$$\rho > 0{\cdot}2\text{–}0{\cdot}3.$$

To extend the range of validity of the expression for K to small values of ρ, we use also the following approximate formula:

$$K = 2{\cdot}96\epsilon^{-1{\cdot}73} - 1{\cdot}96, \tag{1.4}$$

which gives a good approximation for K in (1.3) for $\rho > 0{\cdot}2\text{–}0{\cdot}3$ and tends to unity as $\rho \to 0$. Note that (1.4) is invalid, nevertheless, at very small values of ρ, when K must decrease as $\rho \to 0$ more slowly than the function (1.4). For such values of ρ one can use Tam's (1969) result.

It must be made clear that the functions $K_1(\rho)$ and $K_2(\rho)$ pertain to the force experienced by a rigid random array of particles. The pseudo-turbulent motion of the fluid and particles in the general case influences the interaction force, so that the mean force acting upon real suspended particles involved in pseudo-turbulent pulsations should deviate from (1.2). This is discussed in detail below in § 3.

According to I, a representation for the spectral density of the random concentration fluctuations is needed for closure of equations (1.1). Below we use the representation derived in Buyevich (1970):

$$\left.\begin{aligned} &\Psi_{\rho,\rho}(\omega, \mathbf{k}) = \frac{\mathbf{kDk}}{\pi}\frac{\Phi_{\rho,\rho}(\mathbf{k})}{\omega^2 + (\mathbf{kDk} - T_0\omega^2)^2}, \quad T_0 = \frac{\operatorname{tr}\mathbf{D}}{\langle w'^2\rangle}, \\ &\Phi_{\rho,\rho}(\mathbf{k}) = \int_{-\infty}^{\infty}\Psi_{\rho,\rho}(\omega,\mathbf{k})\,d\omega = \Phi Y(k_0 - k), \\ &\Phi = \frac{3}{4}\frac{\rho^2}{k_0^3}\left(1 - \frac{\rho}{\rho_*}\right), \quad k_0 = \left(\frac{9\pi\rho}{2}\right)^{\frac{1}{3}}\frac{1}{a}, \end{aligned}\right\} \tag{1.5}$$

where $Y(x)$ is the Heaviside step function, $\mathbf{D}$ is the tensor of the pseudo-turbulent diffusivities of particles, $\langle w'^2 \rangle$ is the mean square of the particle pseudo-turbulent velocity, and ω and $\mathbf{k}$ are the frequency and the wavenumber vector, respectively.

In order to give to the reader some idea of the origin of (1.5) we list briefly two key motives leading to this representation. First, the 'local volume concentration' of a monodisperse system can be presented as the sum of certain functions differing only in the values of their arguments. Each function is essentially different from zero only in the close vicinity of some particle centre and marks the location of this particle. It can further be shown that the most detailed and macroscopically meaningful description of the local concentration may be achieved by using the binary correlation function for a dense gas of rigid spheres in this sum. This leads to the above expression for the partial spectral density $\Phi_{\rho,\rho}(\mathbf{k})$ characterizing the random spatial field ρ' at a fixed moment. Second, the dynamics of concentration fluctuations is assumed to be governed by an equation differing from the usual Fick equation. A modified diffusion equation hyperbolic in type is introduced and used while deriving the expression (1.5) for the complete spectral density $\Psi_{\rho,\rho}(\omega, \mathbf{k})$.

This completes the information necessary for the subsequent analysis of the pseudo-turbulent motion and its influence on the mean flow.

2. Pseudo-turbulent diffusion of suspended particles

The spectral density (1.5) of the random process $\rho'(t, \mathbf{r})$ depends substantially upon the tensor $\mathbf{D}$ of the pseudo-turbulent diffusivities of particles, whose components are unknown *a priori*. This fact presents a serious problem in the determination of other statistical characteristics of pseudo-turbulence. It is relevant, therefore, to begin with determination of these components as the first necessary step in the investigation of equilibrium or non-equilibrium properties of the pseudo-turbulent motion under study. Besides, this is of independent interest for evaluation of the efficiency of various transport processes caused by random pulsations of the dispersed phase in fluidized beds and other suspensions commonly encountered in engineering.

2.1. *Representations for the diffusivities*

There exist, in principle, two possible approaches to the problem of particle diffusion. The first one is closely connected with an approximate representation of a cloud of suspended particles as a 'pseudo-gas' of uniform spheres. In this case, while determining the pseudo-turbulent diffusivities of a particle, one may use the well-known methods of the kinetic theory. However, inevitably the question arises as to what extent this analogy is true and, in particular, what type of interparticle interaction must be assigned to the spheres of the pseudo-gas in order to model actual complex interaction between suspended particles.

The second approach is based on an analogy between random pulsations of a particle and those of a fluid element in a turbulent field. This gives an immediate opportunity to express the pseudo-turbulent diffusivities of a particle in just the same manner as the coefficients of turbulent diffusion. Using the efficient

technique developed in the theory of turbulence (see, e.g. Taylor 1921) one can write the following relation for the quantity D_{ij} valid for sufficiently large diffusion times:

$$D_{ij} = \frac{1}{2}\int_0^\infty (C_{wi,wj}(\tau) + C_{wj,wi}(\tau))\, d\tau. \tag{2.1}$$

Here $\mathbf{C}_{w,w}(\tau)$ is the Lagrangian correlation tensor for the pseudo-turbulent fluctuation $\mathbf{w}'$ of the particle velocity and can be defined, in accordance with the treatment in I, as follows:

$$\mathbf{C}_{w,w}(\tau) = \iint e^{i\omega\tau}\, \Psi_{w,w}(\omega, \mathbf{k})\, d\omega\, d\mathbf{k}, \tag{2.2}$$

where integration is performed over all frequencies ω and throughout the entire wavenumber space $\mathbf{k}$. The spectral density tensor $\Psi_{w,w}(\omega, \mathbf{k})$ resulting from equations (1.1) for spectral measures satisfies all the requirements needed for changing the order of the ω and τ integration in the equation obtained by substituting (2.2) into (2.1). On doing this and using the known Fourier transform of Dirac's delta-function we get from (2.1) and (2.2)

$$D_{ij} = \tfrac{1}{4}\pi \int (\Psi_{wi,wj}(0, \mathbf{k}) + \Psi_{wj,wi}(0, \mathbf{k}))\, d\mathbf{k}. \tag{2.3}$$

If one chooses the co-ordinate system so that the axis $x = r_1$ lies along the vector $\mathbf{u}$ marking the axis of the symmetry of pseudo-turbulence in the equilibrium state, then only the diagonal components of the tensors involved in (2.3) are non-zero and this tensor equation is reduced to two scalar equations for the longitudinal ($D_1 = D_{11}$) and the lateral ($D_2 = D_{22} = D_{33}$) diffusivities of a particle.

By solving the equations following from (1.1) at $\omega = 0$ and using the expression (1.2) for the drag force valid at all values of Re, we find that

$$dZ_{wj} = \frac{dZ_\rho}{\beta_1 K + \beta_2(1+\delta_{1j})u}\left\{\beta_1 \frac{dK}{d\rho} u\delta_{1j} + \frac{u}{\epsilon}\frac{k_1 k_j}{k^2} \times [\beta_1 K + \beta_2(1+\delta_{1j})u + \tfrac{4}{3}\nu_0 S k^2 + i\epsilon u k_1]\right\} \quad (\omega = 0).$$

Hence

$$\left.\begin{aligned} \Psi_{w1,w1}(0,\mathbf{k}) &= \frac{1}{\epsilon^2}\left(1+\frac{3{\cdot}5}{150}\frac{Re}{\rho}\right)^{-2}\left\{\left[\frac{d\ln K}{d\rho} + \frac{k_1^2}{\epsilon k^2}\left(1+\frac{3{\cdot}5}{150}\frac{Re}{\rho}+\frac{8}{225}\frac{\epsilon S}{\rho}(ak)^2\right)\right]^2 \right.\\ &\qquad \left. + \left(\frac{1}{75}\frac{ak_1^2}{k^2}\frac{Re}{\rho}\right)^2\right\} u_f^2 \Psi_{\rho,\rho}(0,\mathbf{k}),\\ \Psi_{wj,wj}(0,\mathbf{k}) &= \frac{1}{\epsilon^2}\left(1+\frac{1{\cdot}75}{150}\frac{Re}{\rho}\right)^{-2}\left\{\left(1+\frac{1{\cdot}75}{150}\frac{Re}{\rho}+\frac{8}{225}\frac{\epsilon S}{\rho}(ak)^2\right)^2 \right.\\ &\qquad \left. + \left(\frac{1}{75}\frac{ak_1\epsilon Re}{\rho}\right)^2 \frac{k_1^2 k_j^2}{\epsilon^2 k^4}\right\} u_f^2 \Psi_{\rho,\rho}(0,\mathbf{k}) \quad (j = 2,3). \end{aligned}\right\} \tag{2.4}$$

Here the Reynolds number is given by

$$Re = 2a\nu_0^{-1}u_f, \quad u_f = \epsilon u. \tag{2.5}$$

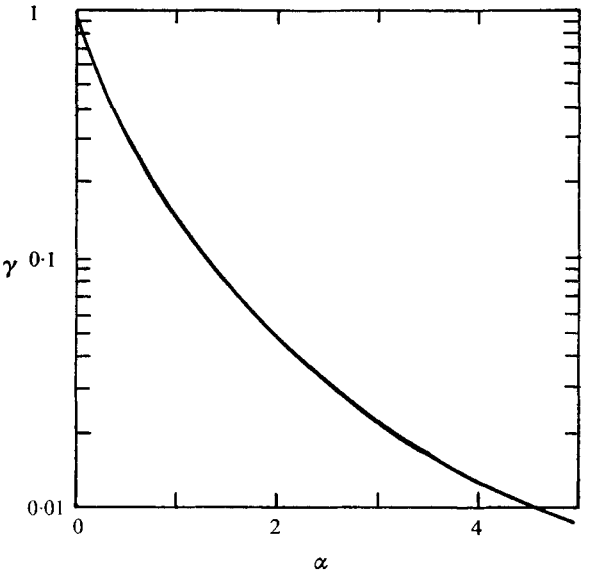

FIGURE 1. Solution of the equation for γ.

No exact expression for the function $S = S(\rho)$ is known at present. However, as has been pointed out in Buyevich & Markov (1970), the terms in (2.4) including this function influence values of the pseudo-turbulent diffusivities corresponding to $Re < 1$ only slightly. One can easily imagine this to be the case also for $Re > 1$. Ignoring the above terms and neglecting the last terms within the curly brackets in (2.4), which are smaller than the corresponding first terms, we obtain finally

$$\Psi_{w1,w1}(0,\mathbf{k}) = \frac{\Phi Y(k_0-k)}{\pi\epsilon^2 k_0^3 \mathbf{kDk}}\left(1+\frac{3{\cdot}5}{150}\frac{Re}{\rho}\right)^{-2}\left[\frac{d\ln K}{d\rho}+\frac{k_1^2}{\epsilon k^2}\left(1+\frac{3{\cdot}5}{150}\frac{Re}{\rho}\right)\right]^2 u_f^2,$$

$$\Psi_{wj,wj}(0,\mathbf{k}) = \frac{\Phi Y(k_0-k)}{\pi\epsilon^4 k_0^3 \mathbf{kDk}}\frac{k_1^2 k_j^2}{k^4}u_f^2 \quad (j=2,3), \tag{2.6}$$

the quantities Φ and k_0 being given by (1.5). Integration of (2.6) using (2.3) leads to equations for the eigenvalues D_1 and D_2 of the tensor $\mathbf{D}$:

$$\left.\begin{aligned} D_1 D_2 &= \frac{2\pi\Phi}{k_0^2}\frac{\gamma^2 u_f^2}{\epsilon^4}(\alpha^2 J_0 + 2\alpha J_2 + J_4), \\ D_2^2 &= \frac{\pi\Phi}{k_0^2}\frac{\gamma^2 u_f^2}{\epsilon^4}(J_2 - J_4), \quad J_n = \int_0^1 \frac{t^n}{t^2+\gamma^2}dt. \end{aligned}\right\} \tag{2.7}$$

Here the following dimensionless parameters have been introduced:

$$\alpha = \epsilon\left(1+\frac{3{\cdot}5}{150}\frac{Re}{\rho}\right)^{-1}\frac{d\ln K}{d\rho} = \frac{1}{\rho+0{\cdot}0233Re}, \quad \gamma = \left(\frac{D_2}{D_1-D_2}\right)^{\frac{1}{2}}. \tag{2.8}$$

Elimination of D_1 and D_2 from (2.7) yields

$$2\alpha^2\gamma^2 J_0 + (4\alpha\gamma^2 - 1 - \gamma^2)J_2 - (1-\gamma^2)J_4 = 0.$$

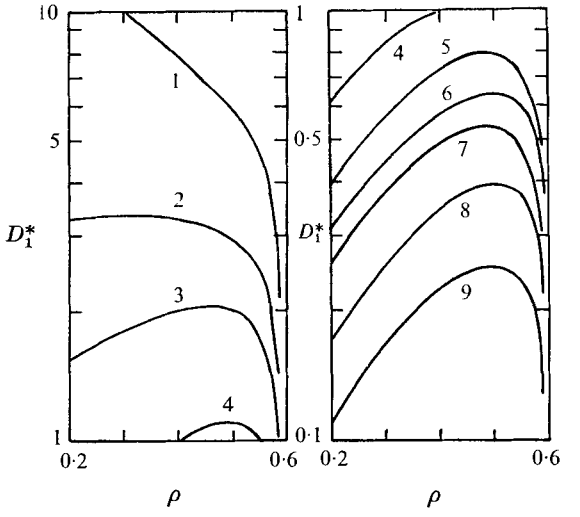

FIGURE 2. Dimensionless longitudinal diffusivity of particles as determined by (2.9). Curves 1–9 correspond to Reynolds number of 0, 10, 20, 40, 60, 80, 100, 200 and ∞ respectively.

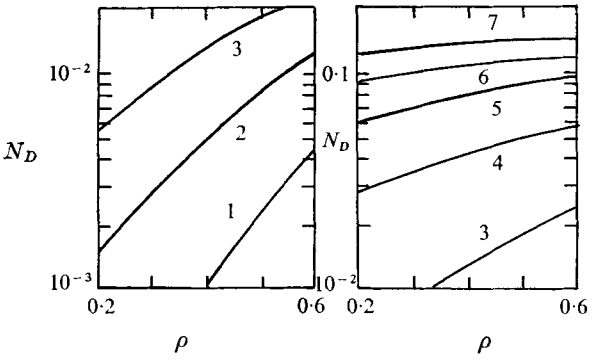

FIGURE 3. Parameter N_D as a function of ρ and Re (nomenclature of the curves is the same as in figure 2).

This equation has a unique positive root, whose dependence upon the parameter α from (2.8) is illustrated by figure 1. The quantities $D_i\,(i = 1, 2)$ are expressed in terms of this root in a following way:

$$\left.\begin{aligned} &D_i = au_f D_i^*, \quad D_2^* = N_D D_1^*, \\ &D_1^* = 0{\cdot}358\frac{\rho^{\frac{2}{3}}}{\epsilon^2}\left(1-\frac{\rho}{\rho_*}\right)^{\frac{1}{2}}\frac{1+\gamma^2}{\gamma}(J_2-J_4)^{\frac{1}{2}}, \quad N_D = \frac{\gamma^2}{1+\gamma^2}. \end{aligned}\right\} \tag{2.9}$$

As $Re \to 0$ these equations reduce to those obtained in Buyevich & Markov (1970). The dependence of the dimensionless parameter N_D and the dimensionless longitudinal diffusivity D_1^* upon ρ at $\rho_* = 0{\cdot}60$ and various values of Re is shown in figures 2 and 3. As can be seen from these figures, D_1^* regarded as a function of ρ has a maximum whose position is displaced to higher values of ρ when Re

increases. The coefficient D_2^* behaves similarly, its maximum at any Re corresponding to a higher value of ρ than that of D_1^*. There is a strong anisotropy in the pseudo-turbulent diffusion of particles which is very well pronounced at small Re but weakens as Re grows. At $Re = 200$ and as $Re \to \infty$ (the corresponding curves are not plotted in figure 3) the quantity N_D is essentially independent of ρ and equals 0·226 and 0·420, respectively. So the longitudinal dispersion of particles in coarse disperse systems is 2·5–5 times as efficient as the lateral dispersion.

2.2. *Comparison with experimental data*

In the literature there is a great number of indirect conclusions concerning particle diffusion in fluidized beds and in other disperse systems under the most different conditions. The main results of the theory, with respect to the general character of the dependence of D_1 and D_2 upon ρ and Re, are in a good qualitative agreement with experimental evidence. However, the number of systematic and, to a degree, exhaustive investigations which could enable us to check the theory quantitatively is rather scarce. This appears to be due to difficulties encountered while attempting to keep track of a particular particle within a concentrated assemblage of many particles and while making a sound interpretation of the data, obtained as a result of cumbersome and complicated experiments.

To confirm the theory from the quantitative point of view, we consider below some results for the longitudinal particle diffusivity derived by Carlos & Richardson (1968) from their experiments with a homogeneous bed of transparent glass beads ($2a \approx 0{\cdot}9$ cm) fluidized by dimethyl phthalate ($\mu_0 \approx 0{\cdot}1$ P). To give a satisfactory interpretation of these results, some discussion of the conditions of the experiments is needed.

The mixing experiments mentioned were performed in two ways. First, a composite bed was formed by placing a horizontal layer of darkened spheres inside the bed before fluidization. An approximate value $D_1^{(1)}$ of the longitudinal mixing coefficient was obtained by comparing the experimental mixing curves for darkened beads with a series of curves derived by solving the Fick's diffusion equation corresponding to different values of $D_1^{(1)}$. Second, the r.m.s. displacement of a tracer particle in the vertical direction was measured and a value $D_1^{(2)}$ of the mixing coefficient was calculated from Einstein's formula

$$\langle (\Delta x)^2 \rangle = 2D_1^{(2)} \Delta t, \tag{2.10}$$

where Δt is the time interval of observation. These methods gave essentially different values for the mixing coefficients.

One can put forward at least two serious objections to the first method. First of all, when the characteristic time of the diffusion process is small enough, the modified hyperbolic diffusion equation has to be applied instead of the usual Fick's equation. This was demonstrated, for example, by Buyevich (1970). In addition (and this is of especial importance), there was a strong circulation flow of the suspended material in the experiments under consideration, so that mixing of darkened beads was caused not only by their pseudo-turbulent diffusion but also by the convective transport resulting from this flow. In fact, the mean velocity W of the upward flow of particles in the central region of the bed was

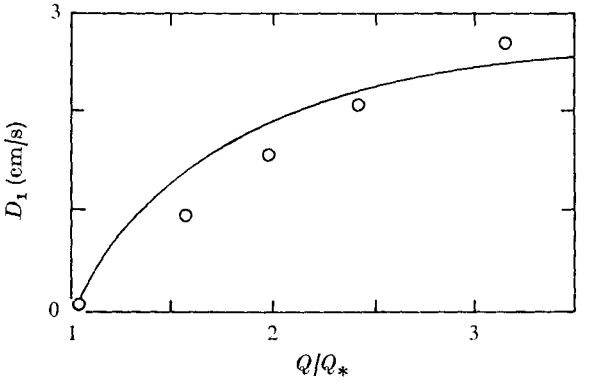

FIGURE 4. Comparison of the theoretical longitudinal diffusivity (solid curve) with experimental data (points) from Carlos & Richardson (1968).

equal to 1–4 cm/s whereas the filtration velocity u_{f*} at the beginning of fluidization was only 4·8 cm/s. The time scale ΔT of the measurements was about 10 s. The convective displacement of a tracer particle during this time was approximately given by $W\Delta T \sim$ 10–40 cm whereas characteristic values of the r.m.s. displacement observed are of order 1–10 cm. Therefore, one has to draw the conclusion that $D_1^{(1)}$ describes the total dispersion of particles due both to convection and to diffusion and can not be used for comparison with the theory.

If the trajectory of a single particle is used while averaging in formula (2.10), then this formula is valid only when Δt exceeds sufficiently the time scale of pseudo-turbulent pulsations and the mean particle velocity W is equal to zero. However, if the averaging is carried out over the trajectories of many particles (i.e. over the ensemble) as seems to have been the case in Carlos & Richardson (1968), then equation (2.10) is adequate for all Δt and $D_1^{(2)} = D_1$. Values of D_1 obtained in such a way at various u_f are shown in figure 4.

The corresponding theoretical curve can be drawn by means of the formulae obtained above. The simple cubic lattice of spheres was used in Carlos & Richardson (1968) as the initial close-packed state of the bed, so that ρ_* has to be put equal to 0·524; the Reynolds number changed from 50 to 160 as the dimensionless parameter u_f/u_{f*} varied in the range 1–3·1. The conformity of the theoretical and experimental results can be regarded as satisfactory.

3. Pseudo-turbulent properties of suspensions at small *Re*

Having the expressions for the components of the diffusivity tensor **D** at our disposal we can find various other characteristics of pseudo-turbulence describing properties of inner local pulsations of both phases from the statistical point of view. To simplify calculations, we consider below, as an example, a suspension of small solid particles ($Re < 1$). Note that pseudo-turbulence in such a system is usually rather weak and therefore can be left out completely in many problems. Nevertheless, in some cases allowance for it is of principal importance (some aspects of this question were discussed in I); knowledge of

pseudo-turbulent quantities is necessary also in the analysis of transport processes.

By introducing the dimensionless spectral measures, frequency and wave-number vector

$$dZ_v^* = \frac{d\mathbf{Z}_v}{u}, \quad d\mathbf{Z}_w^* = \frac{d\mathbf{Z}_w}{u}, \quad dZ_p^* = \frac{dZ_p}{d_0\beta K u a}, \quad \omega^* = \frac{a\omega}{u}, \quad \mathbf{k}^* = a\mathbf{k} \quad (\beta = \beta_1)$$

and taking the parameters $r = Re\,(9K)^{-1}$ and r/κ ($\kappa = d_0/d_1$) to be small compared with unity one can readily demonstrate that equations (1.1) may be replaced in this case by the approximate equations

$$\left.\begin{aligned} -i\mathbf{k}\,dZ_p + d_0\beta K(d\mathbf{Z}_v - d\mathbf{Z}_w) + d_0\beta(dK/d\rho)\,\mathbf{u}\,dZ\rho &= 0, \\ (\omega + uk_1)\,dZ_\rho - \epsilon\mathbf{k}\,d\mathbf{Z}_v &= 0, \\ i\mathbf{k}\,dZ_p + \mu_0 S[k^2 d\mathbf{Z}_v + \tfrac{1}{3}\mathbf{k}(\mathbf{k}\,d\mathbf{Z}_v)] &= 0, \end{aligned}\right\} \tag{3.1}$$

whose solution is

$$\left.\begin{aligned} dZ_p &= \tfrac{4}{3}iSk^2\frac{\omega + uk_1}{\epsilon}\,dZ_\rho, \quad d\mathbf{Z}_v = \frac{\omega + uk_1}{\epsilon}\frac{\mathbf{k}}{k^2}\,dZ_\rho, \\ d\mathbf{Z}_w &= \left[\frac{d\ln K}{d\rho}\,\mathbf{u} + (1 + \tfrac{4}{3}Sk^2)\frac{\omega + uk_1}{\epsilon}\frac{\mathbf{k}}{k^2}\right] dZ_\rho \end{aligned}\right\} \tag{3.2}$$

(we use here the co-ordinate system introduced earlier). By equating S in (3.2) to zero it is easy to obtain simplified expressions for all the spectral measures involved. Note that it would be impossible to take $S = 0$ in (3.1) because they become degenerate in this case.

After a simple calculation we get from (3.2) with $S = 0$ relationships for all the spectral densities of interest, namely,

$$\left.\begin{aligned} \mathbf{\Psi}_{\rho,v}(\omega,\mathbf{k}) &= \frac{\omega + uk_1}{\epsilon}\frac{\mathbf{k}}{k^2}\,\Psi_{\rho,\rho}(\omega,\mathbf{k}), \\ \mathbf{\Psi}_{\rho,w}(\omega,\mathbf{k}) &= \left(\frac{d\ln K}{d\rho}\,\mathbf{u} + \frac{\omega + uk_1}{\epsilon}\frac{\mathbf{k}}{k^2}\right)\Psi_{\rho,\rho}(\omega,\mathbf{k}), \\ \mathbf{\Psi}_{v,v}(\omega,\mathbf{k}) &= \left(\frac{\omega + uk_1}{\epsilon}\right)^2\frac{\mathbf{k}*\mathbf{k}}{k^4}\,\Psi_{\rho,\rho}(\omega,\mathbf{k}), \\ \mathbf{\Psi}_{w,w}(\omega,\mathbf{k}) &= \left[\left(\frac{d\ln K}{d\rho}\right)^2\mathbf{u}*\mathbf{u} + \frac{d\ln K}{d\rho}\frac{\omega + uk_1}{\epsilon}\frac{\mathbf{u}*\mathbf{k} + \mathbf{k}*\mathbf{u}}{k^2}\right. \\ &\qquad \left. + \left(\frac{\omega + uk_1}{\epsilon}\right)^2\frac{\mathbf{k}*\mathbf{k}}{k^4}\right]\Psi_{\rho,\rho}(\omega,\mathbf{k}), \\ \mathbf{\Psi}_{v,w}(\omega,\mathbf{k}) &= \frac{\omega + uk_1}{\epsilon k^2}\left(\frac{d\ln K}{d\rho}\,\mathbf{k}*\mathbf{u} + \frac{\omega + uk_1}{\epsilon}\frac{\mathbf{k}*\mathbf{k}}{k^2}\right)\Psi_{\rho,\rho}(\omega,\mathbf{k}) \end{aligned}\right\} \tag{3.3}$$

(an asterisk designates diadic multiplication). Spectral densities of correlation functions, including the pressure fluctuations, become zero at $S = 0$. By using equation (1.5) for $\Psi_{\rho,\rho}(\omega,\mathbf{k})$ and integrating (3.3) over ω and $\mathbf{k}$ we obtain representations for the statistical characteristics of pseudo-turbulence in the

equilibrium state. These characteristics depend upon the unknown quantity $\langle w'^2\rangle$ involved in (1.5). In particular, we have from equations (2.9)

$$\left.\begin{aligned} \langle w_1'^2\rangle &= \phi\left[\alpha^2+\tfrac{2}{3}\alpha+\frac{1}{5}\left(1+\frac{1+\frac{2}{3}N_D}{1+2N_D}\frac{\langle w'^2\rangle}{u^2}\right)\right]u^2, \\ \langle w_j'^2\rangle &= N_w\langle w_1'^2\rangle = \frac{\phi}{15}\left(1+\frac{1+4N_D}{1+2N_D}\frac{\langle w'^2\rangle}{u^2}\right)u^2 \quad (j=2,3), \\ \phi &= (\rho/\epsilon)^2(1-\rho/\rho_*)^2, \quad \alpha = \epsilon\, d\ln K/d\rho. \end{aligned}\right\} \tag{3.4}$$

An equation for $\langle w'^2\rangle$ follows and yields

$$\langle w'^2\rangle = \phi(\alpha^2+\tfrac{2}{3}\alpha+\tfrac{1}{3})(1-\tfrac{1}{3}\phi)^{-1}u^2. \tag{3.5}$$

This defines completely the expressions (3.4) and the representations for other pseudo-turbulent characteristics as functions of ρ and $\mathbf{u}$. For example, we have

$$\left.\begin{aligned} \langle\rho'\mathbf{v}'\rangle &= M\mathbf{u} = \tfrac{1}{3}\epsilon\phi\mathbf{u}, \quad \langle\rho'\mathbf{w}'\rangle = \epsilon\phi(\alpha+\tfrac{1}{3})\mathbf{u}, \\ \langle v_1'^2\rangle &= \frac{\phi}{5}\left(1+\frac{1+\frac{2}{3}N_D}{1+2N_D}\frac{\langle w'^2\rangle}{u^2}\right)u^2, \\ \langle v_1'w_1'\rangle &= \frac{\phi}{3}\left[\alpha+\frac{3}{5}\left(1+\frac{1+\frac{2}{3}N_D}{1+2N_D}\frac{\langle w'^2\rangle}{u^2}\right)\right]u^2, \\ \langle v_j'^2\rangle &= \langle v_j'w_j'\rangle = \langle w_j'^2\rangle \quad (j=2,3), \\ \langle v_i'v_j'\rangle &= \langle v_i'w_j'\rangle = \langle w_i'w_j'\rangle = 0 \quad (i\neq j). \end{aligned}\right\} \tag{3.6}$$

Note that the expressions (3.4)–(3.6) are very sensitive to the choice of the function $K(\rho)$. To obtain results valid (qualitatively, at least) for all values of ρ within the range 0 to $\rho_* = 0{\cdot}6$ we use further the approximate formula (1.4) in all numerical calculations.

The calculated quantities $\langle w_1'^2\rangle^* = \langle w_1'^2\rangle/u^2$ and N_w regarded as functions of ρ are plotted in figure 5. Figure 6 shows the functions $M(\rho) = \langle\rho'v_1'\rangle^*$ and $\langle v_1'^2\rangle^* = \langle v_1'^2\rangle/u^2$. The dependence of the quantity $\langle v_1'w_1'\rangle/u^2$ upon ρ has the same character and is not plotted. As can be seen from (3.4) and (3.6), the approximate relation $N_v = \langle v_j'^2\rangle/\langle v_1'^2\rangle = \frac{1}{3}(j=2,3)$ holds when $N_D \ll 1$ as is the case for $Re < 1$.

Let us emphasize first that $N_w/N_D \sim 10$, i.e. the effective mixing length for particle diffusion in the longitudinal direction is approximately ten times as high as that for the lateral diffusion. Second, fluid pseudo-turbulent pulsations are weaker and substantially less anisotropic than those of particles.

The pseudo-turbulent normal stresses arising in both phases are of especial interest. According to I and II they are

$$\left.\begin{aligned} P_i^{(p)} &= d_1 L_i^{(p)}u^2, \quad P_i^{(f)} = d_0 L_i^{(f)}u^2 \quad (i=1,2,3), \\ L_1^{(p)} &= \rho\langle w_1'^2\rangle/u^2, \quad L_1^{(f)} = \epsilon\langle v_1'^2\rangle/u^2, \\ L_j^{(p)} &= N_w L_1^{(p)}, \quad L_j^{(f)} = N_v L_1^{(f)} \quad (j=2,3). \end{aligned}\right\} \tag{3.7}$$

The quantities $L_i^{(p)}$ and $L_i^{(f)}$ $(i=1,2,3)$ depend only upon ρ; they are illustrated in figure 7.

Using the above relations one can also evaluate the pseudo-turbulent diffusivities of the fluid in the longitudinal and lateral directions.

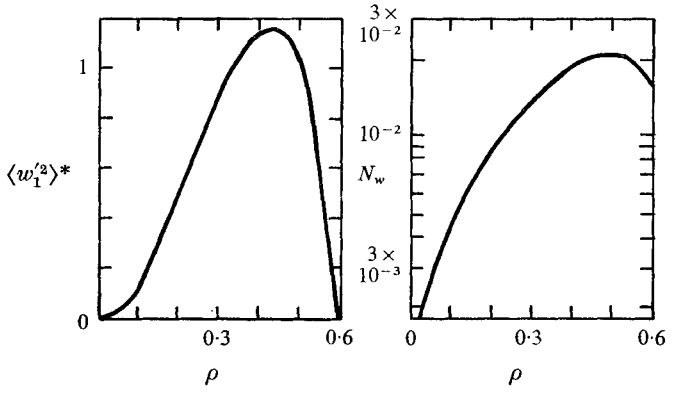

FIGURE 5. Dimensionless parameters $\langle w_1'^2\rangle^*$ and N_w as functions of ρ for $Re < 1$.

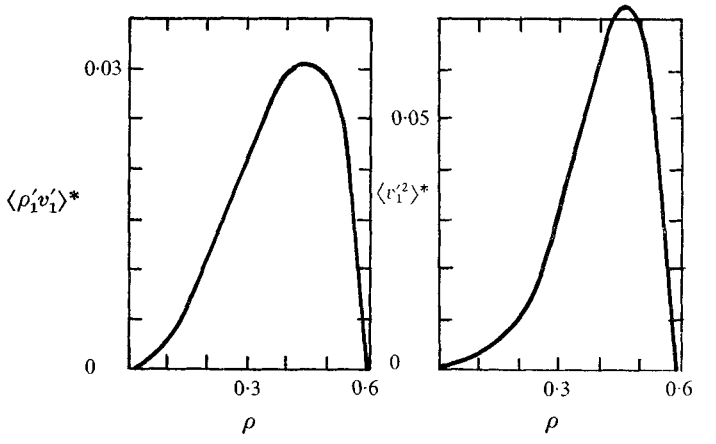

FIGURE 6. Dimensionless parameters $\langle \rho' v_1'\rangle^*$ and $\langle v_1'^2\rangle^*$ as functions of ρ for $Re < 1$.

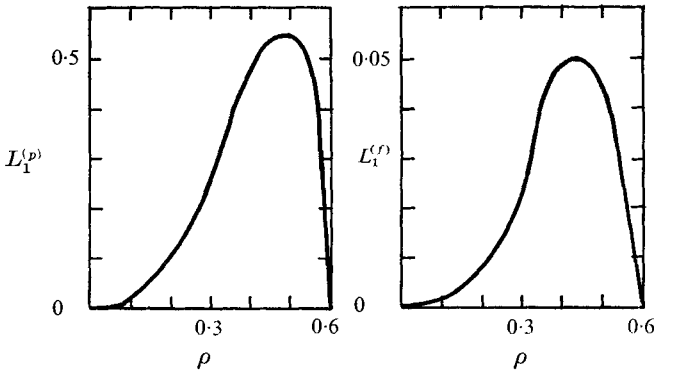

FIGURE 7. Functions determining the pseudo-turbulent normal stresses of both phases.

Unfortunately, the reliable experimental data on equilibrium pseudo-turbulent pulsations available are mostly for systems whose Reynolds number based on the particle radius is not small ($Re \gtrsim 100$). Nevertheless, on considering experimental evidence one may conclude that the character of the dependence of the theoretical values of various pseudo-turbulent characteristics upon ρ and physical parameters of both phases as well as their order of magnitude are confirmed qualitatively by most experiments concerned with pulsations in homogeneous fluidized beds of small particles.

Now we turn to the examination of the effective interaction force between the different phases of a disperse system. As is clear from the treatment in I and II, the mean drag force acting in a real system whose phases are involved in the pseudo-turbulent motion differs from the drag force appearing in a flow of a fluid filtering through an assemblage of immovable particles. Actually, taking the expression for the former force derived in I into account and using the formulae (3.6) we can write the following representation for the mean drag force $\mathbf{f}^0$ per unit volume of the mixture:

$$\left.\begin{aligned} \mathbf{f}^0 = d_0\beta\rho\left[K\mathbf{u} + \frac{dK}{d\rho}\langle\rho'(\mathbf{v}'-\mathbf{w}')\rangle + \frac{1}{2}\frac{d^2K}{d\rho^2}\langle\rho'^2\rangle\mathbf{u}\right] = \lambda_K K\mathbf{u}, \\ \lambda_K = 1-\phi[\alpha^2-(\epsilon^2/2K)\,d^2K/d\rho^2]. \end{aligned}\right\} \tag{3.8}$$

In experiments there is usually determined the function $K^0(\rho)$, which appears in the equation

$$\mathbf{f}^0 = d_0\beta\rho K^0(\rho)\mathbf{u}^0, \tag{3.9}$$

where $\mathbf{u}^0$ is the apparent interstitial velocity of the relative fluid flow caused by the mean flow with the velocity $\mathbf{u}$ and by the additional pseudo-turbulent flux $\mathbf{q} = -\langle\rho'\mathbf{v}'\rangle = -M\mathbf{u}$ (see I). Thus,

$$\mathbf{u}^0 = Q/\epsilon = (1/\epsilon)\,(\epsilon\mathbf{u} - \langle\rho'\mathbf{v}'\rangle) = \lambda_u\mathbf{u}, \quad \lambda_u = 1-\epsilon^{-1}M.$$

So we get by comparing (3.8) and (3.9)

$$K^0 = \lambda_R K, \quad \lambda_R = \lambda_K/\lambda_u. \tag{3.10}$$

This formula enables us to give a natural explanation of the phenomenon of reduced resistance of a fluidized bed observed by many workers (see, e.g. the review in Davidson & Harrison 1963). In fact, according to (3.10) the hydraulic resistance of a fluidized bed whose particles and the fluid phase are involved in pseudo-turbulent motion is somewhat smaller than the resistance of the stationary particulate bed of the same porosity.† The coefficient λ_R in (3.10) plays the role of an effective drag reduction factor for a fluidized bed. λ_R is plotted as a function of ρ in figure 8. It follows from this figure that the reduction discussed can amount to 20 % of the total resistance of the corresponding stationary bed.

† The hydraulic resistance of a stationary bed is influenced to a considerable extent by geometrical properties of its packing, so that various beds of the same porosity may experience essentially different resistance depending on the type of their packing. When comparing the resistance of a fluidized bed with that of a fixed one we refer, of course, only to random arrays of particles characterized by a chaotic manner of packing.

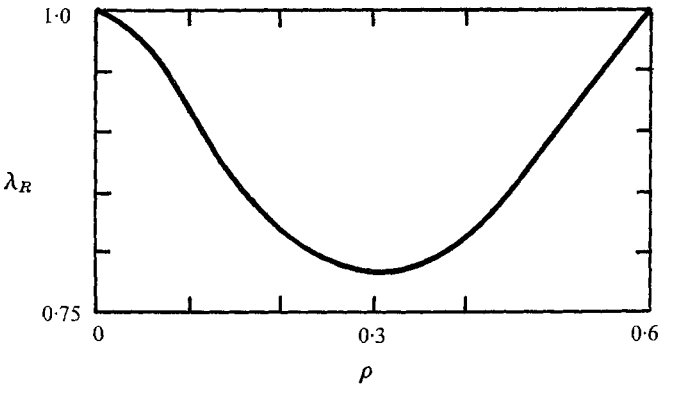

FIGURE 8. Drag reduction factor for a homogeneous fluidized bed.

This effect is due to the fact that the fluid flowing through bed patterns whose porosity is increased because of some fluctuation of the local concentration experiences a smaller hydraulic resistance as compared with the resistance in the stationary particulate bed of the same mean porosity. This decrease in resistance is not completely compensated for by the increase in the resistance force acting upon the fluid flowing through patterns whose porosity is relatively low. This seems to be caused by local rearrangement of a fluid flow within the fluctuating bed, whereby it is just the patterns with higher porosity through which the fluid flows for the most part. Occurrence of the additional fluid flux $\mathbf{q}$ in a disperse system results in a slight additional increase in the apparent hydraulic resistance of the system since $\mathbf{q}$ is negative and the coefficient λ_u^{-1} describing this part of the effect exceeds unity.

This also provides an opportunity to make an indirect quantitative check on the theory even in the case of small Reynolds number. Using values of λ_R shown in figure 8 and Ergun's formula (1.3) for the function $K(\rho)$, one can easily calculate the quantity $K^0(\rho)$ from (3.10). Results of such a calculation are illustrated in figure 9. Additionally, the experimental function $K^0(\rho) = \epsilon^{-2\cdot7}$ for the hydraulic resistance of fluidized beds is plotted in this figure. The exponent $-2{\cdot}7$ in this function is chosen as it is the arithmetic mean of the exponents $-2{\cdot}65$ and $-2{\cdot}75$ suggested in Richardson & Zaki (1954) and Goroshkoh, Rosenbaum & Todes (1958), respectively. (Note that in experiments the function

$$K_d^0(\rho) = \epsilon^{-2} K^0(\rho)$$

is usually determined, cf. (1.3)).

Characteristics of pseudo-turbulence in a non-equilibrium state of a disperse system can deviate substantially from those in the equilibrium state. These deviations can be found by means of the general method developed in I and II. To illustrate this, we confine ourselves to consideration of such deviations from the Navier–Stokes approximation (see II) for the simplest shear flow

$$v = \{u_1, v_2, 0\}, \quad w = \{0, w_2, 0\}, \quad v_2 = \text{constant} + \gamma r_1, \tag{3.11}$$

u_1, u_2, γ and ρ being constant (the component u_1 can appear as a result of action of the external body force).

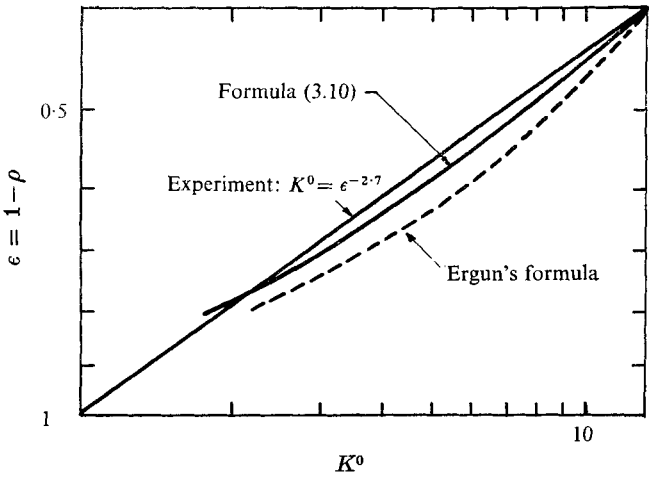

FIGURE 9. Comparison of various functions describing the hydraulic resistence of stationary and fluidized beds at $Re < 1$.

The first step in the calculation of corrections to the equilibrium values of various pseudo-turbulent characteristics consists of determining the first-order correction $\delta\boldsymbol{\theta}$ to the equilibrium tensor $\boldsymbol{\theta} = \langle \mathbf{w}' * \mathbf{w}' \rangle$. After making simple considerations based on results of II we can conclude that the following components $\delta\theta_{12} = \delta\theta_{21}$ appear in the mean flow field (3.11):

$$\delta\theta_{12} = -\frac{\gamma\theta_{11}^0}{4d_0\beta K} = -\frac{\gamma}{4d_0\beta K}(u_1^2 + N_w u_2^2)\langle w_1'^2\rangle^*. \tag{3.12}$$

The superscript zero denotes the quantities related to the equilibrium pseudo-turbulence; N_w and $\langle w_1'^2\rangle^* = u^{-2}\langle w_1'^2\rangle$ are determined in (3.4) and (3.5). The other components of the tensor $\delta\boldsymbol{\theta}$ are zero.

The appearance of the non-diagonal components (3.12) in the flow (3.11) gives rise to tangential stresses $\delta P_{12}^{(p)}$ and $\delta P_{21}^{(p)}$ in the dispersed phase which are expressed in terms of $\delta\theta_{12}$ and $\delta\theta_{21}$ in the same manner as the normal stresses are expressed in terms of $\langle w_i'^2\rangle$ in (3.7). On equating them to $-\eta^{(p)}\gamma$ one obtains the following representation for the pseudo-turbulent shear viscosity of the dispersed phase:

$$\eta^{(p)} = \frac{1}{18}\frac{d_1 a^2}{\mu_0}\frac{L_1^{(p)}}{K}(u_1^2 + N_w u_2^2) \tag{3.13}$$

(here we use the relation (1.2) for $\beta = \beta_1$). The dependence of $\eta^{(p)}$ on the relative fluid velocity u and the physical parameters d_1, a and μ_0 is clear from (3.13); its dependence upon ρ can be easily visualized with the help of figure 7. The stresses $\delta\mathbf{P}^{(p)}$ calculated here do not, of course, describe the stresses resulting from possible dry friction of the surfaces of particles in contact.

In accordance with the method of I and II, the Navier–Stokes correction to the additional fluid flux can be found by means of the relations

$$\delta\mathbf{q} = \mathbf{R}[\rho, \mathbf{v}]\delta\boldsymbol{\theta}, \quad \mathbf{R}[\rho, \mathbf{v}] = \mathbf{q}^0(\boldsymbol{\theta}^0)^{-1}.$$

Keeping in mind that the equilibrium flux $\mathbf{q}^0$ is defined by

$$q_i^0 = -Mu_i \quad (i = 1, 2, 3)$$

we can write

$$R_1[\rho, \mathbf{v}] = -\frac{Mu_1}{\langle w_1'^2\rangle (u_1^2 + N_w u_2^2)}, \quad R_2[\rho, \mathbf{v}] = -\frac{Mu_2}{\langle w_1'^2\rangle (N_w u_1^2 + u_2^2)}, \quad R_3[\rho, \mathbf{v}] = 0$$

and, further, using (3.12),

$$\delta q_1 = \frac{\gamma M u_2}{4d_0 \beta K} \frac{u_1^2 + N_w u_2^2}{N_w u_1^2 + u_2^2}, \quad \delta q_2 = \frac{\gamma M u_1}{4d_0 \beta K}. \tag{3.14}$$

Quite analogously, the tensor $\delta\langle \mathbf{v}' * \mathbf{v}'\rangle$ can be defined as follows:

$$\delta\langle v_i' v_j'\rangle = \tfrac{1}{2}(R_{ik}[\mathbf{v}, \mathbf{v}]\delta\theta_{kj} + R_{jk}[\mathbf{v}, \mathbf{v}]\delta\theta_{ki}),$$

only the diagonal components of the tensor $R_{ij}[\mathbf{v}, \mathbf{v}]$ being different from zero:

$$R_{11}[\mathbf{v}, \mathbf{v}] = \frac{\langle v_1'^2\rangle}{\langle w_1'^2\rangle} \frac{u_1^2 + N_v u_2^2}{u_1^2 + N_w u_2^2}, \quad R_{22}[\mathbf{v}, \mathbf{v}] = \frac{\langle v_1'^2\rangle}{\langle w_1'^2\rangle} \frac{N_v u_1^2 + u_2^2}{N_w u_1^2 + u_2^2},$$

$$R_{33}[\mathbf{v}, \mathbf{v}] = \frac{\langle v_3'^2\rangle}{\langle w_3'^2\rangle} = \frac{\langle v_1'^2\rangle}{\langle w_1'^2\rangle} \frac{N_v}{N_w}.$$

Hence it follows that only the components $\delta\langle v_1' v_2'\rangle = \delta\langle v_2' v_1'\rangle$ of the tensor $\delta\langle \mathbf{v}' * \mathbf{v}'\rangle$ differ from zero. They are expressed in the form

$$\delta\langle v_1' v_2'\rangle = -\frac{\gamma}{8d_0 \beta K} \left(\frac{u_1^2 + N_v u_2^2}{u_1^2 + N_w u_2^2} + \frac{N_v u_1^2 + u_2^2}{N_w u_1^2 + u_2^2} \right) (u_1^2 + N_w u_2^2) \langle v_1'^2\rangle^*. \tag{3.15}$$

Thus, the pseudo-turbulent shear viscosity $\eta^{(f)}$ of the fluid phase is represented in the form similar to that for $\eta^{(p)}$:

$$\eta^{(f)} = \frac{1}{36} \frac{d_0 a^2}{\mu_0} \frac{L_1^{(f)}}{K} \left(\frac{u_1^2 + N_v u_2^2}{u_1^2 + N_w u_2^2} + \frac{N_v u_1^2 + u_2^2}{N_w u_1^2 + u_2^2} \right) (u_1^2 + N_w u_2^2). \tag{3.16}$$

Equations (3.12)–(3.16) are greatly simplified when u_1 or u_2 vanish or when u_1 and u_2 are of the same order of magnitude but $N_w \ll 1$ and so forth. As follows from the analysis in I and II, the expressions for the pseudo-turbulent viscosities of both phases obtained here are valid in the shear flow (3.11) only. The analogous quantities in flows of different structure can be essentially different.

It is evident that, in the general case, the dynamic parameters characterizing the mean flow (i.e. the scalars ρ and p and the vectors $\mathbf{v}$ and $\mathbf{w}$) can not be looked upon as quantities known *a priori*. They must be obtained by solving the equations for the mean motion of both phases of a disperse system, regarded as co-existing interacting continua, under proper boundary conditions. These equations in the Eulerian and Navier–Stokes approximations were considered in detail in II. In order to make this assertion more understandable we consider, by way of example, the situation when the requirement $Q_1 = \varepsilon v_1 + q_1 = 0$ is imposed upon the flow (3.11). This requirement does not mean that the quantity u_1 must vanish. In fact, from the formulae above we have in this case

$$Q_1 = (\varepsilon - M) u_1 + \delta q_1 = 0,$$

the quantity δq_1 depending upon u_1 in accordance with (3.14). This is an equation for the determination of u_1 as a function of the other dynamic variables (i.e. ρ and u_2).

4. Eulerian description of the mean motion of concentrated suspensions

Below we consider some applications of the dynamic equations of the Eulerian approximation derived in II to analysis of the macroscopic behaviour of a disperse system. In the first place, it is expedient to elucidate those features of these equations which lead to the qualitative difference between their solutions and the corresponding solutions of the similar equations in which the pseudo-turbulent stresses in both phases are not accounted for. A simple estimate shows (see e.g. figure 6) that the pseudo-turbulent fluid flux $\mathbf{q}$ is not very important in many cases. Therefore, for the sake of simplicity, we neglect further the corresponding terms in the equations mentioned. Then these equations can be written in the form

$$\left.\begin{aligned}
&\frac{\partial \rho}{\partial t}+\frac{\partial(\rho \mathbf{w})}{\partial \mathbf{r}}=0, \quad \frac{\partial \epsilon}{\partial t}+\frac{\partial(\epsilon \mathbf{v})}{\partial \mathbf{r}}=0,\\
&d_1\rho\left(\frac{\partial}{\partial t}+\mathbf{w}\frac{\partial}{\partial \mathbf{r}}\right)\mathbf{w}=-\frac{\partial \mathbf{P}^{(p)}}{\partial \mathbf{r}}+d_1\rho\mathbf{g}+\mathbf{F}^{(i)},\\
&d_0\epsilon\left(\frac{\partial}{\partial t}+\mathbf{v}\frac{\partial}{\partial \mathbf{r}}\right)\mathbf{v}=-\frac{\partial p}{\partial \mathbf{r}}-\frac{\partial \mathbf{P}^{(f)}}{\partial \mathbf{r}}+d_0\epsilon\mathbf{g}-\mathbf{F}^{(i)},\\
&\mathbf{P}^{(p)}=d_1\rho\langle \mathbf{w}'*\mathbf{w}'\rangle=d_1\mathbf{L}^{(p)}u^2, \quad \mathbf{P}^{(f)}=d_0\epsilon\langle \mathbf{v}'*\mathbf{v}'\rangle=d_0\mathbf{L}^{(f)}u^2,\\
&\mathbf{F}^{(i)}=-\rho\frac{\partial p}{\partial \mathbf{r}}+d_0\rho(\beta_1 K_1^0+\beta_2 K_2^0 u)\,\mathbf{u}.
\end{aligned}\right\} \tag{4.1}$$

Here K_1^0 and K_2^0 are the functions $K_1^0(\rho)$ and $K_2^0(\rho)$ associated with the mean interaction force arising in a real pulsating system, the influence of pseudo-turbulent pulsations upon this force being taken into account. Representations for these functions in terms of K_1, K_2 and various pseudo-turbulent characteristics can be obtained at arbitrary Reynolds number with the help of formulae of I in the same manner as the representation for K^0 has been derived above at small Re. In some cases it is more convenient to regard K_1^0 and K_2^0 as certain empirical functions of ρ without any reference to K_1 and K_2. The pseudo-turbulent normal stresses appearing in (4.1) must be expressed in terms of ρ and $\mathbf{u}$ by means of formulae derived for the equilibrium pseudo-turbulence (e.g. the formulae (3.7) for small Re). Terms describing the effective viscous stresses in the fluid phase which are due to the molecular viscosity of the fluid and proportional to the function $S(\rho)$ are dropped for simplicity. This is certainly consistent with the absence of terms describing the pseudo-turbulent tangential stresses in equations of the Eulerian approximation.

If $u \ll v \sim w$, one can obtain from (4.1) the equations

$$\left.\begin{aligned}
&\frac{\partial \mathbf{v}}{\partial \mathbf{r}}=0, \quad d\left(\frac{\partial}{\partial t}+\mathbf{v}\frac{\partial}{\partial \mathbf{r}}\right)\mathbf{v}=-\frac{\partial p}{\partial \mathbf{r}}-\frac{\partial \mathbf{P}}{\partial \mathbf{r}}+d\mathbf{g},\\
&\mathbf{P}=\mathbf{P}^{(p)}+\mathbf{P}^{(f)}, \quad d=d_0\epsilon+d_1\rho,
\end{aligned}\right\} \tag{4.2}$$

which can be looked upon as the equations for the mean motion of the disperse system itself. However, the relative velocity $\mathbf{u}$, though it is not involved in (4.2), is needed for determination of the pseudo-turbulent normal stresses, so that

solving (4.1) is also necessary. The mean motion of the disperse system can be considered as that of some incompressible homogeneous one-phase fluid only in a trivial case when gradients of $P_i^{(p)}$ and $P_i^{(f)}$ are much smaller than ∇p. However, even in this case the system (4.2) is incomplete because there is no equation for determination of the mean concentration ρ and some independent assumption concerning this quantity has to be made. This has already been discussed in II.

4.1. *Distribution of suspended particles over the height of a homogeneous fluidized bed*

Let us investigate (4.1) for the case when $\mathbf{w} = 0$, $\mathbf{v} = \mathbf{u}(x)$, $\rho = \rho(x)$ and $p = p(x)$, the direction of the x axis being opposite to the vector $\mathbf{g}$. Then we have from the equation of mass conservation of the fluid phase

$$\epsilon \mathbf{u} = \mathbf{Q} = \text{constant}, \tag{4.3}$$

where the total fluid flow $\mathbf{Q} = \mathbf{u}_f$ is regarded as an external parameter defining the state of the system. By excluding dp/dx from the equations of momentum conservation of both phases in (4.1) we get an equation for ρ:

$$d_0 Q \frac{d}{dx}\left(\frac{Q}{\epsilon}\right) = \frac{\epsilon}{\rho}\frac{dP_1^{(p)}}{dx} - \frac{dP_1^{(f)}}{dx} - d_0\left(\beta_1 K_1^0 + \beta_2 K_2^0 \frac{Q}{\epsilon}\right)\frac{Q}{\epsilon} + \epsilon(d_1 - d_0)g. \tag{4.4}$$

Hence, introducing dimensionless parameters and the co-ordinate ξ,

$$\kappa = \frac{d_1}{d_0}, \quad H_1 = \frac{\beta_1 Q}{(\kappa - 1)g}, \quad H_2 = \frac{\beta_2 Q^2}{(\kappa - 1)g}, \quad x = \text{constant} - \frac{Q^2}{(\kappa - 1)g}\xi, \tag{4.5}$$

we obtain finally the following equation governing the spatial distribution of the dispersed phase in the vertical direction:

$$\left.\begin{aligned} \phi(\rho)\frac{d\rho}{d\xi} &= -\psi(\rho) = -\epsilon^3 + \epsilon H_1 K_1^0(\rho) + H_2 K_2^0(\rho), \\ \phi(\rho) &= 1 + \epsilon^2\left[\frac{d}{d\rho}\left(\frac{L_1^{(f)}}{\epsilon^2}\right) - \kappa\frac{\epsilon}{\rho}\frac{d}{d\rho}\left(\frac{L_1^{(p)}}{\epsilon^2}\right)\right]. \end{aligned}\right\} \tag{4.6}$$

Here the representations of the pseudo-turbulent normal stresses in a form similar to that of (3.7) are introduced.

The partial solution of (4.6) describing the uniform distribution of particles is

$$\epsilon_\psi^3 - \epsilon_\psi H_1 K_1^0(\rho_\psi) - H_2 K_2^0(\rho_\psi) = 0, \quad \epsilon_\psi = 1 - \rho_\psi. \tag{4.7}$$

This is an equation determining the concentration $\rho = \rho_\psi$ at given values of H_1 and H_2. In particular, if $Re < 1$, one can drop the last term in (4.7) so that the condition of existence of such a homogeneous distribution has the form

$$\epsilon_*^2 / K_1^0(\rho_*) < H_1 = H < 1, \tag{4.8}$$

where the subscript $*$ denotes quantities related to the state of close packing. If H is less than the quantity on the left-hand side of the inequality (4.8), one has the filtration of fluid through the close-packed particulate bed; if H exceeds unity, isolated particles are brought upwards with the fluid flow. Note that the allowance for the pseudo-turbulent stresses is not essential while considering the uniform spatial distribution.

The function $\psi(\rho)$ in (4.6) decreases monotonously at any κ, H_1 and H_2 while ρ grows from $\rho = 0$ up to $\rho = \rho_*$ and has the unique zero at $\rho = \rho_\psi$, where ρ_ψ is the solution of (4.7). The function $\phi(\rho)$ falls at small ρ ($0 < \rho < \rho_m$) and increases for

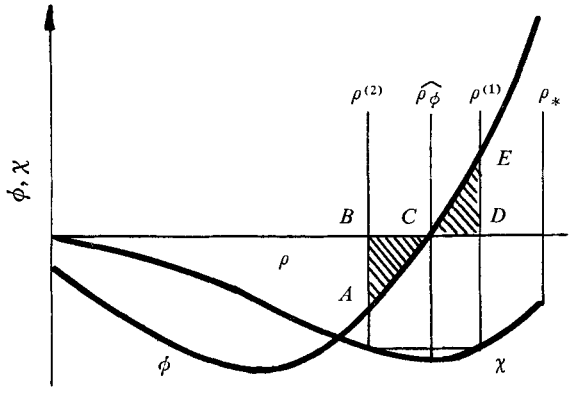

FIGURE 10. Schematic diagram of the functions $\psi(\rho)$ and $\chi(\rho)$.

$\rho > \rho_m$. When $Re < 1$, the function $K_1^0(\rho)$ coincides at small $\rho\,(\rho \ll \rho_*)$ or at $\rho = \rho_* - \delta\rho\,(\delta\rho \ll \rho_*)$ with $K(\rho)$, introduced above, and can be evaluated with the help of the known expressions for the latter function. In the general case one can write

$$K(\rho) \approx 1 + C\rho^{\bar{e}}, \quad \alpha(\rho) \approx \bar{e}C\rho^{\bar{e}-1} \quad (\rho \ll \rho_*).$$

In accordance with Tam's (1969) results $\bar{e} = \frac{1}{2}$ and $C = 3/\sqrt{2}$. Using the relations of the preceding section we have at small Re and ρ

$$L_1^{(p)} \approx \rho^3(\alpha_0^2 + \tfrac{2}{3}\alpha_0 + \tfrac{1}{5}), \quad L_1^{(f)} \approx \tfrac{1}{5}\rho^2, \quad \alpha_0 = \lim_{\rho \to 0} \alpha$$

and, further,

$$\phi \approx 1 - 3\kappa\rho[\alpha_0^2 + \tfrac{2}{3}\alpha_0 + (\tfrac{1}{5} - 2/15\kappa)] \approx 1 - \tfrac{27}{8}\kappa = \phi_0 \quad (\rho \ll \rho_*).$$

So if κ is not small, $\phi < 0$ for $\rho \ll \rho_*$. Similarly, we get near ρ_*

$$\phi \approx 1 + (\kappa\rho_*/e_*)\,[\alpha_*^2 + \tfrac{2}{3}\alpha_* + \tfrac{1}{5}(1 - 1/\kappa)] = \phi_* \quad (\rho_* - \rho \ll \rho_*).$$

Thus, the function $\phi(\rho)$ has a zero at some $\rho = \rho_\phi$ say. The characteristic shape of $\phi(\rho)$ is shown in figure 10. The function

$$\chi(\rho) = \int_0^\rho \phi(\rho)\, d\rho$$

is also plotted in this figure.

If Re exceeds unity, the quantity $\phi(0)$ can, generally speaking, be positive so that the function $\phi(\rho)$ has an additional zero at $\rho = \rho'_\phi$ apart from the zero at $\rho = \rho_\phi$. It is essential that ρ'_ϕ and ρ_ϕ do not depend upon H_1 and H_2.

Now we turn to investigation of the integral curves of equation (4.6) in two cases $\rho_\psi < \rho_\phi$ and $\rho_\phi < \rho_\psi$ at small Re. In both cases we have

$$\rho \approx \begin{cases} |(1-H)/\phi_0|\,(\xi - \xi_0) & \text{for} \quad \rho \ll \rho_*, \\ \rho_* - |\psi(\rho_*)/\phi(\rho_*)|\,(\xi - \xi') & \text{for} \quad \rho_* - \rho \ll \rho_*, \end{cases}$$

where ξ_0 and ξ' are some initial values of the co-ordinate ξ.

(i) $\rho_\psi < \rho_\phi$. Within the region $\rho < \rho_\psi$ one has $\phi < 0$ and $\psi > 0$, so that $d\rho/d\xi > 0$. At $\rho \approx \rho_\psi$

$$\rho = \rho_\psi + \text{constant} \times \exp\,[-|\psi'(\rho_\psi)/\phi(\rho_\psi)|\,(\xi - \xi_0)], \quad \psi' = d\psi/d\rho.$$

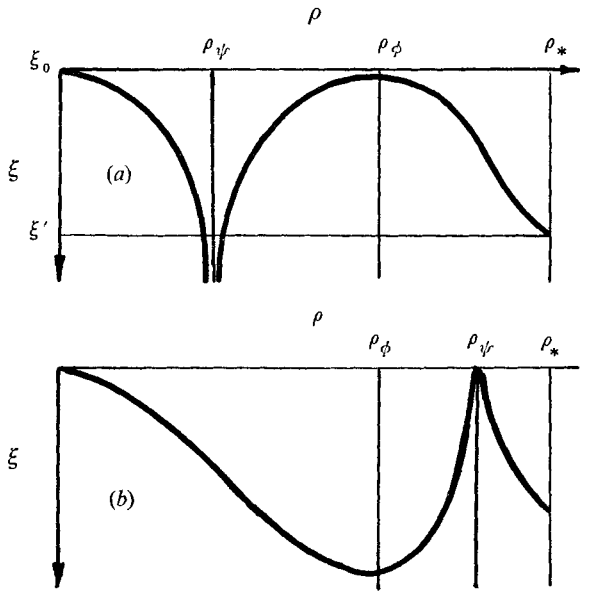

FIGURE 11. Integral curves of equation (4.6).
(*a*) $\rho_\psi < \rho_\phi$; (*b*) $\rho_\psi > \rho_\phi$.

Within the region $\rho_\psi < \rho < \rho_\phi$ the derivative $d\rho/d\xi$ is negative, and is positive for $\rho > \rho_\phi$; at $\rho \approx \rho_\phi$ the quantity ρ is given by

$$(\rho-\rho_\phi)^2 = |2\psi(\rho_\phi)/\phi'(\rho_\phi)|\,(\xi-\xi_0), \quad \phi' = d\phi/d\rho,$$

a prime denoting differentiation with respect to ρ. The characteristic integral curves corresponding to values of ρ_ϕ and ρ_ψ which satisfy the inequality $\rho_\phi < \rho_\phi$ are shown in figure 11 (*a*).

(ii) $\rho_\phi < \rho_\psi$. The analysis is quite similar to that in the case $\rho_\psi < \rho_\phi$. The characteristic integral curves are illustrated in figure 11 (*b*). The trivial solution $\rho = \rho_\psi$ is also shown in this figure.

A real distribution $\rho(\xi)$ may be a continuous function or have discontinuities at some values of ξ. Let one such a discontinuity be at $\xi = \xi^*$, with $\rho(\xi^*_+) = \rho^{(1)}$ and $\rho(\xi^*_-) = \rho^{(2)}$. The values $\rho^{(1)}$ and $\rho^{(2)}$ must satisfy a requirement following from (4.6). We can obtain this requirement by integrating (4.6) over ξ in the region (ξ^*-s, ξ^*+s) and by assuming further that $s \to 0$. We get

$$\chi(\rho^{(1)}) = \chi(\rho^{(2)}), \tag{4.9}$$

the function $\chi(\rho)$ being as defined previously. A pair of values $\rho^{(1)}$ and $\rho^{(2)}$ of ρ meeting this requirement is presented in figure 10. These values are such as to make the shaded areas ABC and CDE on this figure equal.

It is of interest to apply the results obtained to analysis of the distribution of fluidized particles within a homogeneous 'one-dimensional' bed. Choosing the origin $\xi = 0$ at the upper boundary of the bed so that the axis ξ is directed down toward its lower boundary we can obtain, in accordance with integral curves in figure 11, functions $\rho(\xi)$ of two different types. If the total fluid flow Q is large enough and $\rho_\psi < \rho_\phi$, the continuous profile $\rho(\xi)$ presented in figure 12 (*a*) is

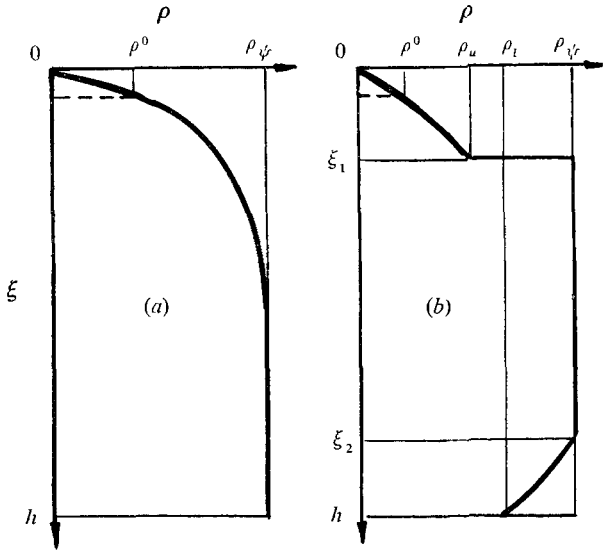

FIGURE 12. Possible distributions of suspended particles within homogeneous fluidized beds. (*a*) $\rho_\psi < \rho_\phi$; (*b*) $\rho_\psi > \rho_\phi$. See text for further explanation.

realized. On the other hand, if Q is comparatively small, i.e. $\rho_\psi > \rho_\phi$, the distribution of fluidized particles is described by a discontinuous function $\rho(\xi)$ whose form is shown in figure 12(*b*). In the former case the real distribution differs from the uniform one corresponding to $\rho = \rho_\psi$ at all ξ although this difference is considerable only within the thin upper region of the bed. In the latter case the fluidized bed consists of three distinct zones. The first zone ($\xi_2 < \xi < h$) is adjacent to a lattice representing the lower boundary of the bed, and ρ increases from some value ρ_l at the lattice up to ρ_ψ at the upper boundary of this zone. The value ρ_l can not be specified within a scope of the Eulerian approximation but it follows from figure 11(*b*) that $\rho_\phi \leqslant \rho_l \leqslant \rho_\psi$. The central zone ($\xi_1 < \xi < \xi_2$) is characterized by the uniform distribution of particles. Finally, within the third zone the concentration falls from ρ_u down to zero, the number ρ_u being connected with ρ_ψ by (4.9).

The total dimensionless height h of the fluidized bed can be found on the basis of the obvious requirement

$$\frac{Q^2}{(\kappa-1)g}\int_0^h \rho(\xi)\,d\xi = V_d, \tag{4.10}$$

where V_d is the known volume occupied by particles of the dispersed phase per unit area of the lower lattice. It is clear that only the central zone of the bed grows when V_d (or h) increases, the other two zones remaining completely unchanged. Obviously, $\xi_1 \sim 1$ and $h - \xi_2 \sim 1$, so that the thickness of the upper and lower zones has the order of magnitude of $(Q^2/g)(\kappa-1)^{-1}$. This quantity can be considerable for beds of coarse particles fluidized by a liquid, when Q is high and κ is of the order of unity.

All these considerations correspond to the function $\phi(\rho)$ being of the same type as the curve plotted in figure 10. If this function has two zeros, then there are additional discontinuities in both profiles in figure 12. That is, the quantity $\rho(\xi)$ does not tend to zero continuously as the upper boundary of the bed is

approached but jumps to zero from the value $\rho = \rho^0$ as can be seen from the dashed lines in figure 12 ($\chi(\rho^0) = 0$).

The discontinuities in the curves in figure 12 are of the same nature as those in solutions of the Eulerian equations for one-phase media. They must vanish when a problem in the next Navier–Stokes approximation is considered. The latter approximation is necessary also for specification of the value ρ_l of the concentration at the lower boundary.

Small as they may be, the pseudo-turbulent normal stresses play a very important role because they influence considerably the very structure of equation (4.6). In fact, when the pseudo-turbulent terms in (4.6) are neglected, we have $\phi = 1$ instead of the previous more complex expression for this function. It can be shown in a quite straightforward way that for $\phi = 1$ equation (4.6) has no solution corresponding to the distribution of a finite number of particles within a finite region in space. In particular, this equation can not be applied in a description of the structure of fluidized bed, if pseudo-turbulence is left out of account.

The distribution of particles within a homogeneous fluidized bed has been measured by many workers (see, for example, Bakker & Heertjes 1960; Kobulov & Todes 1966). The general character of profiles of $\rho(x)$ obtained experimentally is the same as that of the theoretical profiles in figure 12 but one essential difference must be noted. Within the upper part of real fluidized beds there is observed a comparatively long 'tail' of particles, so that $\rho(x)$ tends to zero more slowly than the solutions of (4.6) presented in figure 12. Apparently, this phenomenon is caused by the fact that real particles which are dealt with in experiments are not of the same size and the partial separation of particles occurs in a bed, so that the tail mentioned above is composed mostly of smaller particles.

4.2. *Stability of the uniform flow*

As another example, we consider the stability of the uniform flow

$$\rho = \rho_\psi = \text{constant}, \quad w = 0, \quad v = \{u, 0, 0\}$$

with respect to small disturbances depending upon the vertical co-ordinate x. Taking for simplicity $Re < 1$, we have from (4.7) for $K_2^0 = 0$

$$p = \text{constant} - dgx, \quad u = (\beta K^0)^{-1}\epsilon(\kappa - 1)g, \quad K^0 = K_1^0, \quad \kappa = d_1/d_0. \tag{4.11}$$

Linear equations for small perturbations can be written as follows:

$$\left.\begin{aligned}
&\frac{\partial \rho'}{\partial t} + \rho\frac{\partial w'}{\partial x} = 0, \quad \left(\frac{\partial}{\partial t} + u\frac{\partial}{\partial x}\right)\rho' - \epsilon\frac{\partial v'}{\partial x} = 0,\\
d_1\rho\frac{\partial w'}{\partial t} &= -\rho\frac{\partial p'}{\partial x} + d_0\beta\rho K^0(v' - w') - 2d_1 L_1^{(p)} u\left(\frac{\partial v'}{\partial x} - \frac{\partial w'}{\partial x}\right)\\
&\quad + \left(-\frac{dp}{dx} + \beta u\frac{d(\rho K^0)}{d\rho} - d_1 g\right)\rho' - d_1\frac{dL_1^{(p)}}{d\rho}u^2\frac{\partial \rho'}{\partial x},\\
d_1\rho\frac{\partial w'}{\partial t} + d_0\epsilon\left(\frac{\partial}{\partial t} + u\frac{\partial}{\partial x}\right)v' &= -\frac{\partial p'}{\partial x} - 2d_0 L_1 u\left(\frac{\partial v'}{\partial x} - \frac{\partial w'}{\partial x}\right)\\
&\quad - (d_1 - d_0)g\rho' - d_0\frac{dL_1}{d\rho}u^2\frac{\partial \rho'}{\partial x}, \quad L_1 = L_1^{(f)} + L_1^{(p)}\kappa.
\end{aligned}\right\} \tag{4.12}$$

By putting $$\{\rho, p, v, w\} = \{R, P, V, W\} e^{i(\omega t + kx)}, \tag{4.13}$$
one obtains from (4.12) the system of linear algebraic equations for the amplitudes in (4.13). A necessary condition for existence of a non-zero solution of these equations is

$$\begin{aligned} i\omega^2(d_1\epsilon + d_0\rho) + \omega[2id_0\rho uk + (\rho^{-1} + \epsilon^{-1})(d_0\beta\rho K^0 - 2id_1\epsilon uk L_1^{(p)} + 2id_0\rho uk L_1^{(f)})] \\ + k\left(-\frac{dp}{dx} - \epsilon d_1 g - \rho d_0 g\right) + d_0 uk\frac{\beta d(\rho K^0)}{d\rho} + \frac{uk}{\epsilon}(d_0\beta\rho K^0 - 2id_1\epsilon uk L_1^{(p)} \\ + 2id_0\rho uk L_1^{(f)}) - id_1\epsilon(uk)^2\frac{dL_1^{(p)}}{d\rho} + id_0\rho(uk)^2\frac{dL_1^{(f)}}{d\rho} = 0. \end{aligned} \tag{4.14}$$

It is helpful to simplify (4.14) by using the expressions (4.11) for p and u and by introducing the dimensionless quantities

$$\tilde{\omega} = \frac{\omega}{\beta}, \quad \tilde{k} = \frac{\epsilon}{K^0} akAr, \quad Ar = \frac{(\kappa - 1)g}{\alpha\beta^2}, \quad \kappa = \frac{d_1}{d_0}.$$

Equation (4.14) then becomes

$$\begin{aligned} (\rho + \kappa\epsilon)\tilde{\omega}^2 + \left\{2\left[\left(\rho + \frac{L_1^{(f)}}{\epsilon}\right) - \kappa\frac{L_1^{(p)}}{\rho}\right]\tilde{k} - i\frac{K^0}{\epsilon}\right\}\tilde{\omega} \\ + \left[\rho\left(\frac{dL_1^{(f)}}{d\rho} + \frac{L_1^{(f)}}{\epsilon} + 1\right) - \kappa\epsilon\left(\frac{dL_1^{(p)}}{d\rho} + \frac{L_1^{(p)}}{\epsilon}\right)\right]\tilde{k}^2 - i\rho\frac{K^0}{\epsilon}\left(2 + \epsilon\frac{d\ln K^0}{d\rho}\right)\tilde{k} = 0. \end{aligned} \tag{4.15}$$

The uniform flow (4.11) will be stable to infinitesimal perturbations (4.13) if the imaginary parts of all the roots of (4.15) are positive. Keeping this in mind we obtain after a simple calculation a condition of infinitesimal stability in the form

$$\kappa T_1(\rho) - T_2(\rho) > 0, \tag{4.16}$$

where

$$\left.\begin{aligned} T_1(\rho) &= \epsilon(dL_1^{(p)}/d\rho + L_1^{(p)}/\epsilon) - 2L_1^{(p)}f - \epsilon\rho^2 f^2, \\ T_2(\rho) &= \rho(dL_1^{(f)}/d\rho + L_1^{(f)}/\epsilon + 1) - 2\rho(\rho + L_1^{(f)}/\epsilon)f + \rho^3 f^2, \\ f(\rho) &= 2 + \epsilon\, d\ln K^0/d\rho. \end{aligned}\right\} \tag{4.17}$$

It is interesting that (4.16) does not involve the dimensionless number $\tilde{k}$, i.e. the flow (4.11) is stable or unstable to disturbances of all wavelengths simultaneously. It can be easily demonstrated by using the above representations for $L_1^{(p)}$ and $L_1^{(f)}$ that the function $T_2(\rho)$ is always positive (here we restrict attention to the case $Re < 1$, of course). Therefore, the condition (4.16) can not be satisfied no matter what the concrete value of κ if $T_1(\rho) < 0$. However, (4.16) could be valid if $T_1(\rho) > 0$ and

$$\kappa > \kappa_0(\rho) = T_2(\rho)/T_1(\rho). \tag{4.18}$$

A simple estimate shows the function $T_1(\rho)$ to be positive for sufficiently small ρ and negative for $\rho \sim \rho_*$. In particular, it follows from (3.7) and (4.18) that

$$\kappa_0(\rho) = 1/\rho[2\alpha_0(\alpha_0 - 1) - \tfrac{17}{5}], \quad \alpha_0 = \lim_{\rho\to 0}\alpha, \quad \rho \ll \rho_*,$$

α being defined by (3.4). On calculating α in accordance with Tam's (1969) formula one obtains $\alpha_0 \approx \frac{3}{2}(2\rho)^{-\frac{1}{2}}$ and $\kappa_0(\rho) \approx \frac{4}{9}$, so that the instability occurs only when κ is smaller than $\frac{4}{9}$. For $\kappa > \frac{4}{9}$ the flow (4.11) is stable relative to infinitesimal disturbances of arbitrary wavelength.

Thus, accounting for pseudo-turbulent stresses leads to a result which is qualitatively new as compared with results of known investigations of stability of

two-phase disperse flows to infinitesimal perturbations, random pulsations of both phases being neglected (see e.g. Jackson 1963; Murray 1965; Pigford & Baron 1965). In fact, such investigations allow the conclusion to be made that disperse two-phase flows are always unstable. This point of view was confirmed also by stability analysis in Crowley (1971), where the problem of the disrupting of a layer of particles moving through a viscous fluid into clusters of particles separated by open channels was treated microscopically. In contrast, brief as it may be the above analysis shows that the pseudo-turbulent motion exerts a substantial stabilizing influence which is of especial importance at small ρ. A similar opinion concerning the influence of the 'pressure' of the dispersed phase upon the infinitesimal stability was expressed by Anderson & Jackson (1968). However, they assumed this pressure to be isotropic and nothing definite was said about its dependence upon ρ and other dynamic variables describing the mean motion whose stability was investigated.

These examples of application of the conservation equations governing the macroscopic behaviour of a disperse system are by no means exhaustive. Nevertheless, they indicate the great influence on properties of the mean flow which is caused by pseudo-turbulence, however weak it may be. These equations (even in the simplest Eulerian approximation) involve essential nonlinearities and serious mathematical difficulties may be encountered while attempting to formulate boundary conditions appropriate for various particular problems concerned with disperse systems and to solve the corresponding boundary problems. However, one can certainly expect results of such an approach to be suggestive and revealing in the matter of qualitative conclusions and order-of-magnitude calculations.

I would like to thank Dr Otto Chubanov for his assistance in the numerical calculation.

REFERENCES

Anderson, T. B. & Jackson, R. 1968 *Ind. Engng Chem. Fund.* **7**, 12.

Bakker, P. J. & Heertjes, P. M. 1960 *Chem. Engng Sci.* **12**, 260.

Buyevich, Yu. A. 1970 *Zh. Prikl. Mekh. Tekhn. Fiz.* no. 6.

Buyevich, Yu. A. 1971 *J. Fluid Mech.* **49**, 489.

Buyevich, Yu. A. 1972 *J. Fluid Mech.* **52**, 345.

Buyevich, Yu. A. & Markov, V. G. 1970 *Zh. Prikl. Mekh. Tekhn. Fiz.* no. 1.

Carlos, C. R. & Richardson, J. F. 1968 *Chem. Engng Sci.* **23**, 813, 825.

Crowley, J. M. 1971 *J. Fluid Mech.* **45**, 151.

Davidson, J. F. & Harrison, D. 1963 *Fluidised Particles.* Cambridge University Press.

Ergun, S. 1952 *Chem. Engng Progr.* **48**, 89.

Goroshkoh, V. D., Rosenbaum, R. B. & Todes, O. M. 1958 *Izv. Vysshykh Uchebnykh Zavedenii, Neft i Gas*, no. 1.

Jackson, R. 1963 *Trans. Instn Chem. Engrs*, **41**, 13.

Kobulov, V. G. & Todes, O. M. 1966 *Zh. Prikl. Khim.* **39**, 1075.

Murray, J. D. 1965 *J. Fluid Mech.* **21**, 465.

Pigford, R. L. & Baron, T. 1965 *Ind. Engng Chem. Fund.* **4**, 81.

Richardson, J. F. & Zaki, W. N. 1954 *Trans. Instn Chem. Engrs*, **32**, 35.

Tam, C. K. W. 1969 *J. Fluid Mech.* **38**, 537.

Taylor, G. I. 1921 *Proc. Lond. Math. Soc.* **20**, 196.